Comparative Study of Mg-Si Films Deposited by DC- and RF- Glow Discharge Sputtering

SERIKAWA Tadashi*, KAWABATA Kenshi and KONDOH Katuyoshi*****

Abstract

Mg-Si thin films were deposited at low substrate temperature by direct current (DC)- and radio frequency (RF)- glow discharge sputtering from targets composed of Mg and Si plates with area ratios of 25%:75% and 50%:50%. X-ray diffraction measurements clarified that films deposited by both DC- and RF- glow discharge sputtering from the target of Mg:Si =25%:75% showed the intermetallic compound magnesium silicide (Mg_2Si). Structural, mechanical, and corrosion-resistance properties of Mg-Si films deposited from the target of Mg:Si =25%:75% were examined. The films for both DC- and RF- sputtering showed stack structures consisting of crystalline Mg_2Si layers with columnar and amorphous phase layers. However, the amorphous phase layer for an RF-sputtered film was shown to be much thicker than that for the DC-sputtered film. Mechanical properties of elastic modulus and hardness measured by the nano-indentor method for RF-sputtered films were higher than those for DC-sputtered films. Corrosion-resistance tests in a 5% sodium spray test showed that RF-sputtered films also had superior corrosion-resistance properties to DC-sputtered films. These mechanical and corrosion-resistance properties are strictly caused by the crystalline property and film structure of sputtered Mg-Si films. In this paper, the properties of DC- and RF- sputtered films are also discussed together with film deposition.

KEY WORDS: (Glow Discharge) (Direct Current (DC-) Sputtering**) (**Radio Frequency (RF-) Sputtering**) (**Intermetallic Compound**) (**Magnesium Silicide (Mg_2Si)**)** (Mg-Si Thin Films)

1. Introduction

The intermetallic compound magnesium silicide, Mg_2Si, has attracted much interest as a narrow-gap semiconductor and environmentally friendly material.[1-6] Moreover, the Mg_2Si has also been found to show a possibility for application to structural components because of excellent mechanical properties and high corrosion-resistance.[7,8] However, formation of Mg_2Si film is difficult because of very high vapor pressure and low condensation coefficient of magnesium.[9] This is probably one reason that studies of the Mg_2Si films are scarce, though several attempts have been made. One of these is a fabrication process utilizing magnesium reaction with silicon substrates by high temperature annealing of silicon substrate in Mg vapor.[10,11] Another is using Mg_2Si films formed on silicon substrates by molecular-beam epitaxy precisely controlling magnesium and silicon flux ratios and substrate temperature.[2-4] Recently, the fabrication process of Mg_2Si films at low substrate temperature by ion beam sputtering was developed.[12,13] . However, ion beam sputtering method has the disadvantage of not being applicable to mass production of thin films, compared with glow discharge sputtering. Glow discharge sputtering in both direct current (DC-) and radio frequency (RF-) modes has advantages for mass production, and, has been widely used in the industrial field for formation of various kinds of metal, semiconductor and insulator films.

In this study, Mg-Si films were deposited at low substrate temperature by DC- and RF- glow discharge sputtering. Deposition and film properties were comparably studied and discussed.

2. Experimental

Figure 1 shows a schematic diagram of the glow dischage sputtering system used in this study. The glow discharge sputtering chamber consists of a substrate loading room and a film deposition room. A glow discharge electrode of planar magnetron cathode with sputtering target is set in the film deposition room. A target is fixed on the planar magnetron cathode. The substrate loading tray carries substrates between the substrate loading room and the film deposition room. Glow discharge plasma is generated by applying direct current (DC) and 13.56 MHz radio frequency (RF) power to the electrode. **Figure 2** shows photographs of targets with area ratios of Mg:Si=50%:50% (a) and 25%:75% (b). Rectangle shaped targets of 70 mm x 200 mm and 5 mm thickness consists of Mg and Si plates, as shown in the figure. The Mg and Si plates are alternately arranged

† Received on December 14, 2007
* Appointment Researcher
** Research Associate
*** Professor

Transactions of JWRI is published by Joining and Welding Research Institute, Osaka University, Ibaraki, Osaka 567-0047, Japan

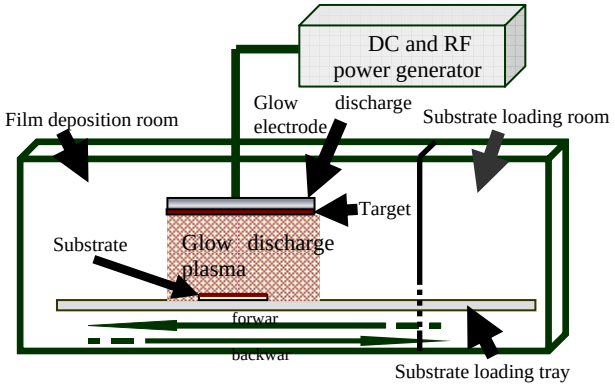

Fig.1 Schematic diagram of glow discharge sputtering system used in this study.

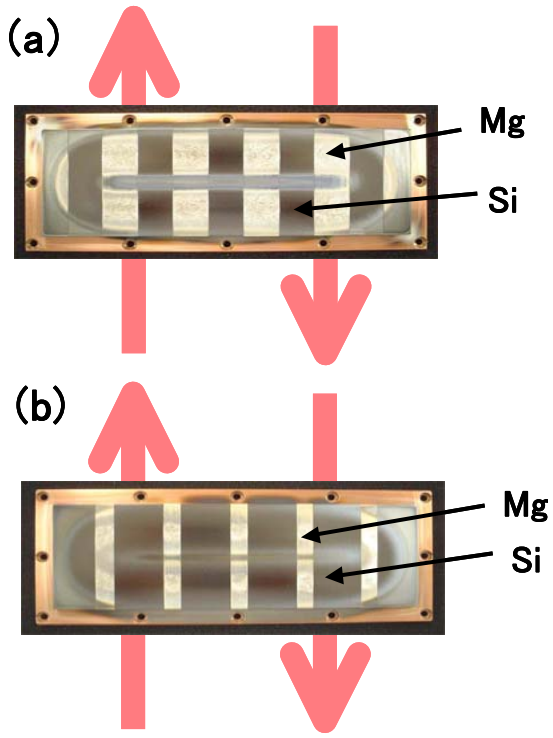

Fig.2 Photograph of targets composed of Mg and Si with area ratio of Mg:Si=25% : 75% (a) and =50%:50% (b). Arrows in the figures refer to directions of substrate movement against the targets.

and are fixed to Cu sheet by soldering. The Cu sheet with Mg and Si plates was mechanically clamped to a water-cooled planar magnetron cathode. The planar magnetron cathode was fed with DC- and RF- power to generate glow discharge plasma.

First, the sputtering chamber was evacuated to less than 1 x 10^{-4} Pa pressure, then, argon gas of 99.999 % purity was introduced to the chamber. The argon gas pressure was adjusted at 0.51 Pa. Glow discharge plasma was generated by supplying DC- and RF- power. The powers were set at 100 W and 200 W for DC- and RF-glow discharge sputtering, respectively. Glass and copper plates of 18 mm x 18 mm square and 0.2 mm thickness were used as substrate. The substrate was carried into the sputtering room by moving the substrate tray. Thin films were deposited during substrate moving in forward and backward directions in the glow discharge plasma, as shown in Fig.1. In Fig.2, the moving direction of the substrate against the target is also indicated. In this study, depositions of 1 μ m thick films were prepared through two times of forward- and backward-moving of the substrate in the sputtering plasma. Substrate temperature was maintained lower than 100 ℃. **Table 1** shows film deposition conditions.

Structural, mechanical, and corrosion-resistance properties of films deposited on glass substrate were evaluated. Crystal and structural properties were examined by transmission electron microscopy (TEM), electron diffraction and X-ray diffraction (XRD) methods. Compositions of the films were measured by X-ray fluorescence spectroscopy (XRF). Films for measurements of composition were deposited on copper substrates.

Mechanical properties of elastic modulus and hardness of the films deposited on glass substrate were measured by a dynamic nano-indentator (MTS NanoIndentor (TestWork-4)(XP/DCM)). The maximum indentation displacement was set at 430 nm. This leads to a maximum indentation load of approximately 16 mN. The elastic modulus and hardness of the films were calculated from the load-displacement data following the method proposed by Oliver and Pharr.[14)]

Table 1 Film deposition conditions

Glow discharge mode	Target Mg:Si =	Power	Sputtering gas pressure	Substrate temperature	Pass times under the target
DC sputtering	50%:50%	100 W	0.51 Pa	below 100℃	4 times
	25%:75%				
RF sputtering	50%:50%	200 W	0.51 Pa		
	25%:75%				

3. Results and Discussion

3.1 Mg-Si film depositions

Mg concentration in the film was measured by an XRF method. Films were deposited on copper substrate by DC- and RF-sputtering from targets of Mg:Si= 50%:50% and 25%:75%. Film composition was obtained by comparison with measured Mg concentration of bulk materials of metallic compound magnesium silicide Mg_2Si. Measurements indicated 82-85 at.% Mg concentrations for the 50%Mg-50%Si target and 58-66 at.% for 25%Mg:75%Si one. The Mg concentration in film from 25%Mg:75%Si targets is nearer to 67 at.% of stoichiometric intermetallic compound Mg_2Si. Moreover, DC- and RF- sputtered Mg-Si films have almost the same film composition. Crystal properties of Mg-Si film were measured by the X-ray diffraction (XRD) method. **Figures 3 (a)** and **(b)** shows XRD patterns of films from targets of Mg:Si =25%:75% for DC- and RF- glow discharge sputtering. XRD patterns for both sputtered films have almost the same features as each other. Very broad peaks near $2\theta = 24^\circ$ and many sharp peaks are observed for both films. The very broad peaks are due to the amorphous phase in Mg-Si film and substrate glass. Sharp peaks at $2\theta = 24^\circ$ and 39° are from the crystal Mg_2Si film structure. Small peaks in DC-sputtered film (a) at $2\theta = 47^\circ$ and 73° are also attributed to crystal Mg_2Si film structures. It should be noticed that a metallic Mg peak were not observed in the XRD patterns for either DC- or RF-sputtered films. Therefore, the XRD patterns indicate that magnesium silicide Mg_2Si films were formed by DC- and RF- sputtering from the target of Mg:Si =25%:75%.

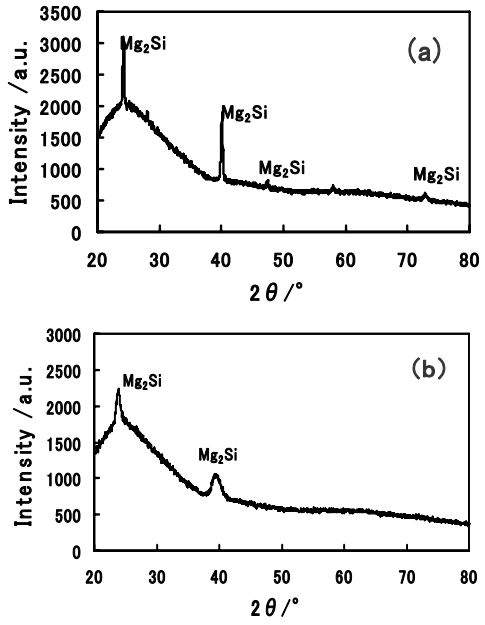

Figs.3 (a), (b) X-ray diffraction patterns for thin films deposited by DC- (a) and RF- (b) glow discharge sputtering from the target with area ratio of Mg:Si=25%:75%.

3.2 Mg-Si film structure

Figures 4 and **5** show photographs of cross-sectional transmission electron microscopy (TEM) for the films by DC- and RF- sputtering from the target of Mg:Si =25%:75%. The films shows almost stoichiometric compositions of the intermetallic compound Mg_2Si, as mentioned above. In the figures, electron diffraction patterns at positions pointed out in the TEM photograph are also shown. The figures clearly indicate that films have four-layer structures for both DC- and RF-sputtering. These four-layer structures are caused by the double time of forward- and- backward passing in the glow discharge plasma as shown in Fig.1. However, the film structure of each layer in DC- and RF- sputtered films is different. In the DC-sputtered film, a very thin amorphous phase is formed near the interface between layers and a crystalline phase in almost the total area of all layers, as shown in Fig.4. On the other hand, electron diffraction patterns for RF-sputtered film (Fig.5) indicate that amorphous and crystalline phases are formed in the bottom and upper regions in the first, second and third layers, respectively. As shown in Figs. 4 and 5, crystalline phases in both DC- and RF-sputtered films are composed of grains with columnar structure. Columnar structure for the DC-sputtered film is coarse compared with the RF-sputtered film.

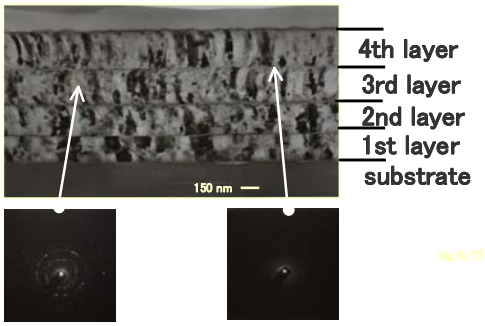

Fig.4 Photographs of cross-sectional transmission electron microscopy (TEM) and electron diffraction patterns for film deposited by DC-glow discharge sputtering.

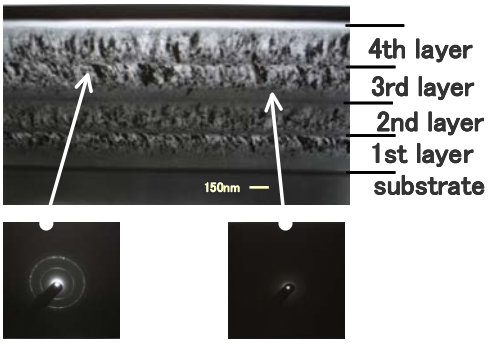

Fig.5 Photographs of cross-sectional transmission electron microscopy (TEM) and electron diffraction patterns for film deposited by RF-glow discharge sputtering.

It is well known that compressive film stress is

developed in sputter-deposited film from high energy particle bombardment.[15] It is also known that compressive stress is accumulated in the film with increasing film thickness in ion-beam sputter-deposited Mg-Si films. [12] When the film stress reaches at critical level, transition of amorphous to crystalline Mg_2Si phases occurs. As shown in Fig.5 for the RF-sputtered film, the stress assisted transitions in the first, second, and third layers are caused through the same mechanism as in ion-beam sputter-deposition. However, the fourth layer has enough accumulated stress to form a crystalline phase even at initial stages of film growth, resulting in the formation of crystalline phases in almost the total area of the fourth layer. On the other hand, all layers in DC-sputtered films are composed of crystalline phase as shown in Fig.4. Moreover, the columnar structure is coarse compared with RF-sputtered films. This may be due to large film stress in DC-sputtered films compared with RF-sputtered films. However, film stress is intensively influenced by deposition condition (e.g. substrate temperature, fluxes of Mg and Si atoms) but also the bombarding of high energy particles of Ar-ion and electrons. To clarify the difference of film stress between DC- and RF- sputtered Mg-Si films, intensive studies of the film deposition are needed.

3.3 Mechanical properties of Mg-Si film

Glow discharge sputtered Mg-Si films have amorphous and crystalline phases mixed structure, as shown in Figs. 4 and 5. It was also demonstrated that amorphous Mg-Si films show a mechanical property of good durability for wear resistance compared with crystalline Mg-Si films.[8] Mechanical properties of elastic modulus and hardness for glow discharge sputtered Mg-Si films were measured by a dynamic nano-indentator. **Figures 6 (a)** and **(b)** show profiles of elastic modulus and hardness with displacement within the indentation depth up to 400 nm for films by DC- and RF- sputtering from the target of Mg:Si=25%:75%. For comparison, mechanical properties of quartz substrate were also measured at same conditions as the Mg-Si films. As shown in figure, both resulting elastic modulus and hardness of quartz material reaches constants of 72 GPa and 9.5 GPa at 50 nm depth. On the other hand, elastic modulus and hardness for the DC- and RF-sputtered Mg-Si films show behaviors of increasing up to 50 nm depth and after this depth, gradually decreasing to constant values of 80 GPa and 5.8 GPa, respectively. In the depth region smaller than 50 nm, both mechanical properties for RF-sputtered film are higher than those for DC-sputtered films. These differences in mechanical properties between DC- and RF-sputtered films result from the Mg-Si film structure shown in Figs. 4 and 5, that is, the amorphous phase in RF-sputtered films raises the mechanical properties.

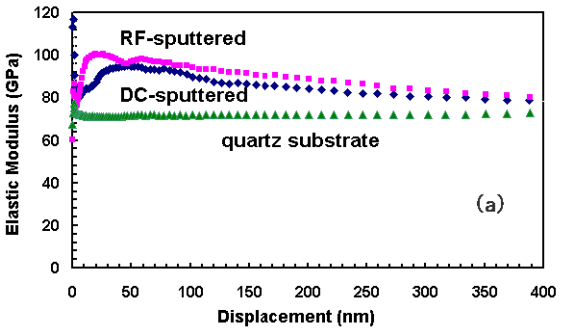

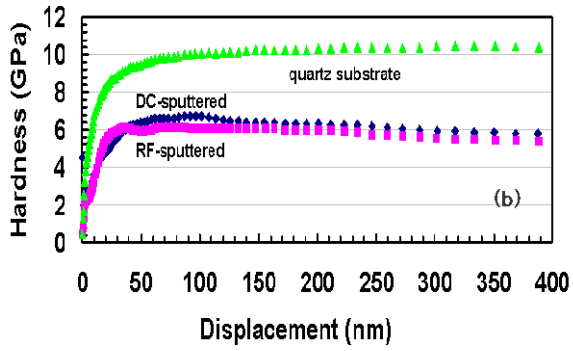

Figs.6 (a), (b) Mechanical properties of elastic modulus (a) and hardness (b) for films deposited by DC- and RF-glow discharge sputtering. Elastic modulus and hardness for quartz material are also plotted.

3.4 Corrosion-resistance property of Mg-Si film

The salt spray test (5%Nacl at 308K) (SST) on DC-and RF-sputtered Mg-Si films was carried out for up to 100 hours. The films were deposited on glass substrates from targets of Mg:Si=25%:75% and 50%:50%. Results are summarized in **Table 2** as parameters of spraying time. Symbols of ○, △ and X in the table mean no corrosion, partial corrosion and fully removing of film, respectively. The films from the 50%Mg:50%Si target are fully removed even at one hour of spraying time. This is due to excess metallic Mg in the Mg-Si film mentioned in previous section. For films from the 25%Mg:75%Si target, the RF-sputtered film shows superior corrosion-resistance property to the DC-sputtered film. This high corrosion resistance property of the RF-sputtered film is caused by amorphous phases in the Mg-Si film shown in Fig.5. On the other hand, the poor corrosion-resistance property for the DC-sputtered film is due to crystalline property and coarse columnar film structure shown in Fig.4.

Table 2 Corrosion-resistance properties

Sputtering Conditions		Spraying time (hours)							
Glow discharge mode	Target Mg:Si =	1	3	6	12	24	48	72	100
Direct Current (DC)	25%:75%	○	○	△	△	△	△	△	—
Radio frequency (RF)	50%:50%	X	X	X	X	X	X	X	—
	25%:75%	○	○	○	○	○	○	○	○

4. Conclusions

Mg-Si films were deposited on glass substrates by DC- and RF- glow charge sputtering using the target composed of Mg and Si plates with Mg:Si=50%:50% and 25%:75% area ratios. Films having the intermetallic compound Mg_2Si were successfully formed from the target of Mg:Si=25%:25% for both sputtered films. Structural, mechanical and corrosion-resistance properties of the films were measured. DC-sputtered Mg-Si films are composed of very thin amorphous phases and crystalline phases with coarse columnar. On the other hand, RF-sputtered film shows layered structures of thick amorphous phases and crystalline phases with fine columnar structure. Nano-indentor measurements indicated that mechanical properties of elastic modulus and hardness for RF-sputtered film are higher than those for DC-sputtered film. Moreover, the corrosion-resistance property for the RF-sputtered film is superior to that of the DC-sputtered film. Differences of these mechanical and corrosion-resistance properties between DC- and RF-sputtered films are mainly caused by the crystalline properties and film structure.

Acknowledgments

The authors would like to thank Momoko Henmi for her help in thin film depositions. This study was financially supported by the matching foundation project by Ministry of Education, Culture, Sports, Science and Technology of Japan.

References

1) J.Tejeda and M.Cardona, Physical Review B-condensed matter, **14(6)** (1976) 2559.
2) A.Vantomme, J.E.Mahan, G.Langouche, J.P.Becker, M.V.Bael, K.Temst, and C.V.Haesendonck, Appl. Phys. Lett., **70 (9)** (1997) 1086.
3) J.H.Hhan, A.Vantomme, and G.Langouche, Physical Review B- condensed matter, **54 (23)** (1996) 16965.
4) T.Kajikawa, K.Shida, K.Shiraishi., T.Ito, M.Omori, and T.Hirai, Proceeding of the 16th Internationl Conference on Thermoelectronics (IEEE, Inc., Picscataway, NJ, 1997) 362.
5) P.L.Janega, J.McCaffrey, D.Landheer, M.Buchanan, M.Denhoff, and D.Mitchwel, Appl. Phy. Lett., **53** (1988) 2056.
6) H.Matsui, M.Kuramoto, T.Ono, Y.Nose, H.Matsuoka, and H.Kuwabara, J.Crytal. Growth, **237-239** (2002) 2121.
7) K.Kondoth, T.Yamaguchi, T.Serikawa, and H.Oginuma, The 2nd JSME/ASME International Conference on Material and Processing 2005-The 13th JSME Materiala and Processing Conference (M&P 2005)-(June 19-22, 2005, Seattle, USA).
8) T.Yamaguchi, T.Serikawa, M.Henmi, H.Oginuma, and K.Kondoh, Material Transaction, **47** (2006) 185.
9) Selected Values of the Thermodynamic Properties of the Elements, edited by R.Hultgren (American Society of Metals, Metal Park, Ohio (1973)).
10) M.Wittmer, W.Luthy, and M.Von.Allmen, Phys. Lett., **75A** (1979) 127.
11) T.Hosono,Y.Matsuzawa, M.Kuramoto, Y.Momose, H.Tatsuoka, and H.Kuwabara, Solid State Phenomena, **93** (2003) 447.
12) T.Serikawa, M.Henmi, and K.Kondoth, J. Vacuum Science and Technology A, **22** (2004) 1971.
13) T.Serikawa, M.Henmi, T.Yamaguchi, H.Ogimura, and K.Kondoh, Surface and Coatings Technology, **200** (2006) 4233.
14) W.C.Oliver and G.M.Pharr, J. Mater. Res. **1** (1992) 613.
15) J.A.Thornton, J.Tabock, and D.W.Hoffman, Thin Solid Films, **64** (1979) 111.